THE JOURNAL OF PHYSICAL CHEMISTRY B

Article

pubs.acs.org/JPCB

Understanding the Interaction between Valsartan and Detergents by NMR Techniques and Molecular Dynamics Simulation

Chenyu Cao,[†,‡] Jiezhen Mao,[‡] Fang Li,[§] Minghui Yang,[‡] Hongqing He,[*,‡] Ling Jiang,[*,‡] and Maili Liu[‡]

[†]School of Life Science and Technology, Huazhong University of Science and Technology, Wuhan, 430074, China

[‡]Wuhan Center for Magnetic Resonance, State Key Laboratory of Magnetic Resonance and Atomic and Molecular Physics, Wuhan Institute of Physics and Mathematics, Chinese Academy of Sciences, Wuhan, 430071, P.R. China

[§]Department of Chemistry, Central China Normal University, Wuhan, 430079, P.R. China

Supporting Information

ABSTRACT: Valsartan (VST) is one of the Angiotensin II receptor antagonists, which is widely used in clinical hypertension treatment. It is believed that VST incorporates into biological membranes before it binds to AT_1 receptor. Herein the interactions between VST and detergents, mimicking the membrane environment, were investigated by using nuclear magnetic resonance (NMR) techniques and molecular dynamics (MD) simulation. We observed that VST has two conformers (trans and cis) exchanging slowly in DPC (dodecyl-phosphocholine) micelles, a widely used detergent. The changes of chemical shifts, relaxation rates, and self-diffusion coefficients of VST protons indicate that both conformers have strong interactions with DPC. NOE cross peaks and MD simulation reveal that DPC interacts with VST not only through the hydrophobic lipid chain, but also the hydrophilic headgroup, locating VST at the charged headgroup and upper part of the micelles. Our results are in good agreement with the Raman spectroscopic studies of VST in the DPPC (dipalmitoyl-phosphatidylcholine) bilayers by Potamitis et al. (*Biochim. Biophys. Acta.* **2011**). The concentration ratio of trans over cis conformers is 0.94, showing that two conformers have the same affinities with the detergent, which is significantly smaller than our previous results obtained in SDS (sodium dodecyl sulfate) micelles. MD simulation suggested that the cis conformer has slightly lower binding free energy than the trans conformer when interacting with DPC. The conformational change of VST was further investigated in two detergents, CTAB (hexadecyltrimethylammonium bromide) and Tween-20 (polysorbate 20). Ratios of conformer A and B in the presence of detergents are in the order of DPC, CTAB < Tween-20 < SDS, which is correlated with the charge characters of their head groups. NMR investigations and MD simulations indicate that the electrostatic interaction plays an essential role in the binding process of VST with detergents, and the hydrophobic interaction influences the packing of the drug in the micelles. These results may be of help in understanding delivery processes of sartan drugs in cell membranes.

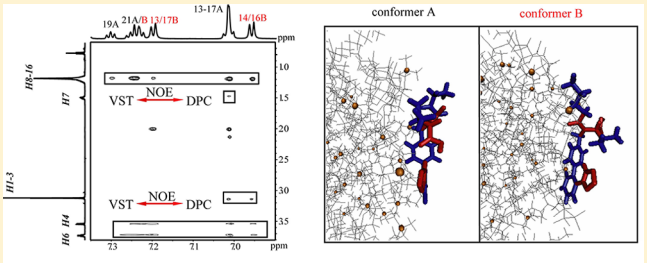

INTRODUCTION

Valsartan (VST) is one of the Angiotensin II receptor antagonists, which is widely used in clinic to prevent hypertension. It modulates the renin-angiotensin system (RAS) by binding with type I Angiotensin II receptor (AT_1) with high affinity, the combined effect of which is reduction of blood pressure.[1] Recently, it has been found that VST lowers brain β-amyloid ($A\beta$) protein levels and improves spatial learning in a mouse model of Alzheimer,[2] making it a promising drug to prevent and even treat Alzheimer's disease.[3] AT_1 receptors are members of the G protein-coupled receptors family consisting of seven transmembrane helices.[4,5]

A two-step model is widely accepted as the mechanism of sartan antagonist binding to AT_1 receptor.[6] It suggests that the drug penetrates into the cell membrane and then interacts with AT_1 receptor. Thus, phospholipid membranes are expected to play a key role in drug delivery. For this reason, the thermal, dynamic, and structural effects of sartan drugs on phospholipid bilayers have been studied through the combination of various techniques. Theodoropoulou et al. used differential scanning calorimetry (DSC), electron spin resonance (ESR) spectroscopy and ^{31}P nuclear magnetic resonance (NMR) spectroscopy to investigate how losartan affects the thermotropic behavior and molecular mobility of phosphatidylcholine and phosphatidylethanolamine bilayer membranes. The results showed that losartan incorporates in lipid bilayers and locates itself close to the interfacial region of the phosphatidylcholine (DMPC and DPPC) bilayers at lower concentrations and deeper within the bilayers at higher concentrations.[7] The interactions of losartan with phosphatidylethanolamine (DMPE, DPPE and DEPE, respectively) membranes are more superficial than with phosphatidylcholine bilayers.[8] Recently, Mavromoustakos's group has done a lot of extensive investigations on a series of tetrazole-based sartan drugs within the lipid bilayers by using

Received: May 3, 2012
Revised: May 30, 2012
Published: June 18, 2012

dx.doi.org/10.1021/jp304304v | *J. Phys. Chem. B* 2012, 116, 7470−7478

DSC, Raman, and solid state ^{31}P NMR spectroscopies et al. Results indicated that losartan anchors in the mesophase region of the DPPC bilayers with the tetrazole group oriented toward the polar headgroup, whereas candesartan has less definite localization.[9] Meanwhile, losartan exerts stronger interactions compared with candesartan as depicted by the more prominent thermal, structural, and dipolar ^{1}H−^{31}P changes that are caused in the DPPC bilayers. Furthermore, SAXS measurement showed that losartan's action is more likely to take place in fluid plasma membrane patches such as palmitoyl-oleoyl-phosphatidylcholine (POPC) bilayers rather than in domains rich in cholesterol and saturated lipid species such as DMPC bilayers.[10] ^{13}C CP/MAS spectra provided direct evidence for the incorporation of olmesartan and cholesterol in DPPC bilayers and showed both olmesartan and cholesterol are residing at the headgroup region and upper segment of the lipid bilayers. However, they display distinct impacts on the bilayers' properties due to their different sizes. Olmesartan is the only sartan antagonist so far studied that increases the gauche:trans ratio in the liquid crystalline phase.[11] The interactions between valsartan and DPPC bilayers have also been studied by Raman spectroscopy which indicated that VST localized at the charged head groups and upper part of the DPPC bilayers.[12]

All of these sartan drugs show high silmilarities in their interactions with lipid bilayers; however, most of the studies focus on the changes of membranes, whereas the influences on the drug itself caused by the interactions have not been thoroughly discussed. Herein, the conformational change of VST and interactions between VST and detergents were investigated by NMR spectroscopy and molecular dynamics (MD) simulation. Detergents are amphipathic molecules usually consisting of a polar or charged headgroup and an extended hydrophobic hydrocarbon chain (Chart 1). The detergent molecules cooperatively assemble into micelles when the concentration is above the critical micelle concentration (CMC). They are widely used to mimic cell membrane for studying membrane proteins and the interaction between membranes and proteins.[13,14] NMR is a powerful technique to study the molecular interaction. Chemical shifts,[15] line widths, and relaxation times[16,17] of ^{1}H NMR spectrum are sensitive to the changes of chemical environments in solution. Self-diffusion coefficient can be also measured from ^{1}H NMR experiments and provides direct evidence of the molecular size.[18]

Chart 1. Molecular Structures of VST and Different Detergents[a]

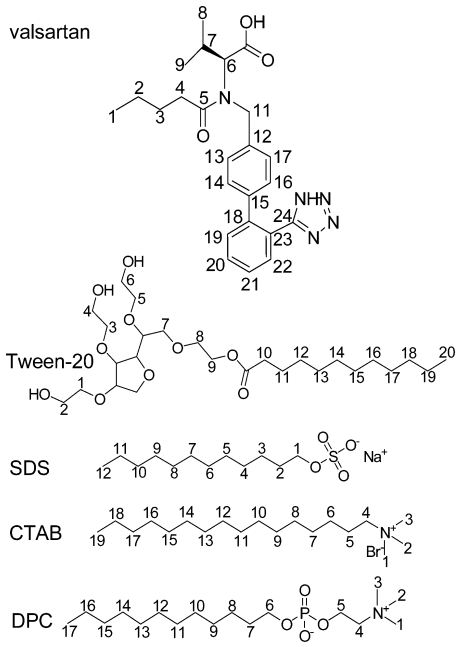

[a]Five dihedral angles of VST are defined as: τ1 = C18−C23−C24−N(H), τ2 = C19−C18−C15−C14, τ3 = C13−C12−C11−N, τ4 = C12−C11−N−C6, and τ5 = C6−N−C5−O.

In our previous work,[19,20] we found that VST has two conformers (A, trans and B, cis) exchanging slowly on NMR time scale through the rotation of the C(O)−N bond (Chart 1) both in solution and SDS micelles. In aqueous solution, the concentration ratio of A to B is 0.88, whereas in the SDS micelles the ratio increases to 1.49. MD simulations revealed that the hydrophobic interaction is the predominant effect and conformer A has more concentrated hydrophobic center that makes it easier to insert into SDS micelles. Here, the interaction between DPC (dodecylphosphocholine) and VST was studied by the same techniques. VST shows two sets of NMR signals in the presence of DPC, corresponding to conformers A and B in methanol and SDS micelles by Li et al.[19,20] and trans and cis conformers in DMSO by Potamitis et al.[21] Interestingly, two conformers have similar binding affinities with DPC micelles and the concentration ratio of conformer A to B is 0.94. Considering the different charges of the head groups of DPC and SDS, we recorded the experiments of VST in other detergents, which are cationic detergent CTAB (hexadecyltrimethylammonium bromide) and nonionic detergent Tween-20 (polysorbate 20). It has been found that the concentration ratio of conformer A to B is highly correlated to the charge of head groups of these detergents. NOE measurements were also used to provide intermolecular binding information between VST and detergents. The NMR results and MD simulations suggest that VST interacts with detergents through not only hydrophobic interactions but also electrostatic interactions. These results give us insight of the binding process, which help understanding of the mechanism of VST inserting into biological cell membranes.

EXPERIMENTAL METHODS

Sample Preparation. Dodecylphosphocholine (DPC, 99%) was purchased from Avanti Polar Lipids. Deuterated dodecylphosphocholine (d38-DPC, 98%) was from Cambridge Isotope Laboratories incorporated. Sodium dodecyl sulfate (SDS, 99%) was from Alfa Aesar (Johnson-Matthey Company). Hexadecyltrimethylammonium bromide (CTAB, 99%) and polysorbate 20 (Tween-20, 99.8%) were purchased from Acros Organics (New Jersey, U.S.A.). All of these reagents were used without any further purification. Valsartan (VST, (*S*)-*N*-valeryl-*N*-((2′-(1H-tetrazol-5-yl)-biphenyl-4-yl)-methyl)-valine) was purified according to the published method.[22]

All of the NMR samples were prepared in 20 mM phosphate buffer, 100% D_2O, with a final pD at 7.4. Two groups of VST samples were prepared, with and without 200 mM d38-DPC. The concentrations of VST are 1.0, 2.0, 3.0, 4.0, 5.0, 6.0, 7.0, 8.0, 10.0, 12.0, and 15.0 mM. We also prepared a group of samples containing 15.0 mM VST and different detergents, 200 mM DPC, 10 mM CTAB, 10 mM Tween-20, and 200 mM SDS.

NMR Spectroscopy. The NMR experiments of VST and VST-d38-DPC sample sets were performed at 298 K on the

dx.doi.org/10.1021/jp304304v | J. Phys. Chem. B 2012, 116, 7470−7478

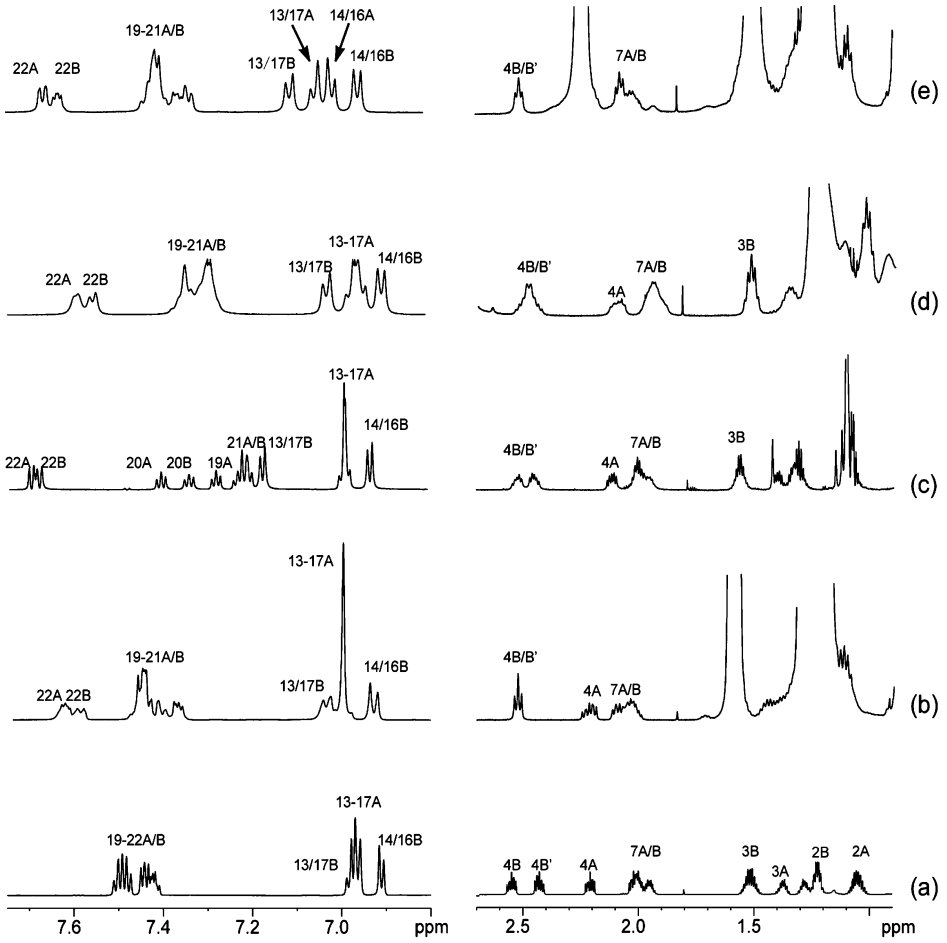

Figure 1. Expansion of ^{1}H NMR spectra of 15.0 mM valsartan in phosphate buffer (pH 7.4) (a), 200 mM SDS (b), 200 mM d38-DPC (c), 10 mM CTAB (d), and 10 mM Tween-20 (e).

Bruker AVANCE instruments with a proton frequency of 600.13 MHz equipped with a 5 mm triple-resonance cryoprobe. The NMR experiments of samples containing 15.0 mM VST in various detergents were recorded at 500.13 MHz with a 5 mm probe at room temperature.

^{1}H NMR spectra were acquired using a solvent presaturation sequence with a spectra width of 8000 Hz, 32 scans, and 64 000 data points. Longitudinal relaxation times (T_1) and transversal relaxation times (T_2) were measured by using conventional inversion recovery and CPMG pulse sequences, respectively. ^{1}H−^{14}N HSQC[23] spectra were conducted using a modified ^{1}H−^{15}N HSQC pulse sequence with four scans, 1024 data points in F2, and 64 data points in F1. The INEPT evolution time was optimized to be 16.7 ms, corresponding for J_{NH} of 7.5 Hz, for both CH_3 and CH_2O proton detection. A double multispin echo (DMSE)[24] experiment with bipolar gradient pulses was used to determine the self-diffusion coefficients (D). The effective diffusion time is 360 ms. NOESY spectra were acquired by a WATERGATE W5[25] water suppressed NOESY sequence with 48 scans, 4096 data points in F2, and 300 data points in F1. The mixing times are 200 ms for all of the samples.

Molecular Dynamic Simulations. All MD simulations were performed using the AMBER 10.0 package,[26] and a GAFF force field[27] was employed. Both DPC and SDS micelles were constructed with 60 surfactant molecules.[28,29] 60 Na^+ counterions were added to balance the negative charges of sulfate groups in SDS micelles. The geometries of VST and the partial charges between micelle and VST were calculated as described previously[19,20] with the Gaussion 09 software package[30] and the restrained electrostatic potential (RESP) method.[31]

Four MD trajectories were produced for VST_A-DPC, VST_B-DPC, VST_A-SDS, and VST_B-SDS. The systems were minimized for 20 000 steps. The first 5000 steps were in the steepest descent method and then 5000 steps in the conjugate gradients method under weak harmonic constraints on VST molecule with spring constants of 10 kcal/(mol·Å^2). Another 10 000 step minimization was with all constraints relaxed. These systems were all heated to 300 K in 50 ps in NVT ensemble and then subjected to NPT dynamics (pressure P = 1 atm and temperature T = 300 K) for 20 ns. The simulation parameters were the same as in our previous studies,[20] except that the cutoff for the nonbonded interactions was reduced to 10 Å. PTRAJ module in AMBER 10.0 was used to analyze the trajectories, and the VMD program[32] was used in the visualization.

Free Energy Calculations. The absolute binding free energies (ΔG_{bind}) of two systems (VST-DPC and VST-SDS) can be calculated using the MM/PBSA procedure according to

$$\Delta G_{bind} = G_{complex} - (G_{receptor} + G_{ligand}) \quad (1)$$

where $G_{complex}$, $G_{receptor}$, and G_{ligand} represent the free energies of complex, receptor, and ligand averaged over snapshots taken from MD trajectories. We treated the whole micelle as the

dx.doi.org/10.1021/jp304304v | J. Phys. Chem. B 2012, 116, 7470−7478

receptor and the VST molecule as the ligand. The snapshots, equally spaced at 20 ps intervals, were culled from the MD trajectories and gave 200 snapshots for 4 ns.

The binding free energy contains an enthalpic and an entropic contribution

$$\Delta G_{\text{bind}} = \Delta H - T\Delta S \quad (2)$$

The enthalpy of binding ΔH is composed of the sum of molecular mechanical (MM) energy (ΔG_{MM}) and the solvated free energy contribution (ΔG_{solv}). The ΔG_{solv} can be divided into a polar ($\Delta G_{\text{solv-polar}}$) and nonpolar ($\Delta G_{\text{solv-nonpolar}}$) part. The polar contribution $\Delta G_{\text{solv-polar}}$ was calculated by solving the Poisson–Boltzmann (PB) equations for nonzero salt concentrations as implemented in Delphi II.[33] In Delphi calculations, the grid spacing was set to 4 Å, and the radii of atoms were taken from the PARSE parameter set.[34] The values of the interior dielectric constant and the exterior dielectric constant were set to 1 and 80, respectively. The nonpolar solvation energy $\Delta G_{\text{solv-nonpolar}}$ was calculated from the solvent-accessible surface area (SASA) using the MSMS program,[35] with a probe radius of 1.4 Å, according to the equation

$$\Delta G_{\text{solv-nonpolar}} = \gamma \text{SASA} + \beta \quad (3)$$

where the surface tension γ and the offset β were set to the standard values of 0.00542 kcal mol^{-1} Å^{-2} and 0.92 kcal/mol, respectively.

RESULTS AND DISCUSSIONS

1. Interaction between VST and DPC. The interactions between VST and DPC were investigated by measuring proton chemical shifts, relaxation times, and molecular self-diffusion coefficients. The ^{1}H NMR resonances of VST in the absence and presence of DPC are unambiguously assigned by using one- and two-dimensional (1D and 2D) NMR spectroscopy. In all of the experiments, except NOESY, d38-DPC was used instead of DPC to reduce the overlap of ^{1}H NMR spectrum.

Chemical Shift Analysis. The expanded ^{1}H NMR spectra of 15.0 mM VST in the absence and presence of DPC are shown in Figure 1, panels a and c. VST shows two sets of ^{1}H resonances (conformer A and B), which is in agreement with our previous studies.[19,20] Chemical shift drifting and line broadening can be clearly observed with the addition of DPC. Such as the overlapped proton resonances of H19–22 at 7.45 ppm become well-resolved and spread around 7.2–7.7 ppm. The peaks at 2.4–2.6 ppm, donated as H4 resonances of conformer B, became broad and started to immerge. The proton chemical shifts versus VST concentration are illustrated in Figure 2. The chemical shifts of two sample groups showed

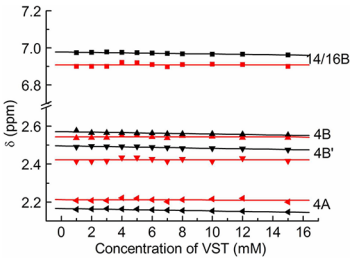

Figure 2. ^{1}H chemical shifts of VST (δ) as a function of VST concentrations in phosphate buffer (red) and 200 mM d38-DPC (black).

no dependence on the VST concentration. The addition of DPC caused downfield chemical shift changes of the phenyl protons H14/16, and upfield change of the methylene protons H4 in conformer A and downfield change of H4 in conformer B. It means that the aromatic and aliphatic parts of VST are both involved in the interaction and experience different chemical environment in DPC micelles.

^{1}H–^{14}N HSQC experiment has been successfully applied in the investigation of choline-containing compounds.[23] The choline group of DPC gave three peaks in the ^{1}H–^{14}N HSQC spectra assigned as methyl and methylene resonances. They showed the same chemical shifts at 48.0 ppm along the ^{14}N dimension. The proton chemical shifts were 4.21 ppm (H5), 3.63 ppm (H4), and 3.19 ppm (H1–3) (numbered in Chart 1), respectively, and shifted to 4.19, 3.59, and 3.17 ppm after the addition of 15.0 mM VST. The changes provided direct evidence that VST interacts with the choline head groups.

Proton Relaxation Time. The interactions between VST and DPC are further investigated by measuring the proton relaxation times. T_1 and T_2 of both sample groups are not sensitive to the drug concentration (Table S1). After the addition of DPC, the relaxation times of H4 protons for conformers A and B reduced by almost the same amplitude, showing no conformation selectivity. Specifically, T_2 values of H4 and H14/16 protons both reduced by approximately 80% because of a restricted motion in the micelles. However, T_1 values of H4 protons reduced by about 7% and those of H14/16 protons reduced by about 16%, indicating that the aromatic parts of VST binds more tightly with the detergent.

Self-diffusion Coefficient. Self-diffusion coefficient (D) of the molecules in solution can be measured by PFG-NMR experiment. It represents the molecular mobility that is relative to the viscosity of the solution and the spherical size of the particles. D is a good parameter to estimate the binding affinity of VST to the micelles. When detergents were added, the D value of VST represented an apparent self-diffusion coefficient D_{obs}, which is a weighted average coefficient of the bound VST D_{b} and free VST D_{f} in equilibrium state. It can be described simply by an equation

$$D_{\text{obs}} = X_{\text{b}}D_{\text{b}} + (1 - X_{\text{b}})D_{\text{f}} \quad (4)$$

where X_{b} represents the molar ratio of the bound VST and the solvent viscosity η can be estimated by the Stokes–Einstein equation[36]

$$D = \frac{KT}{6\pi\eta r} \quad (5)$$

where K represents Boltzmann constant, T represents the absolute temperature, and r represents the radius of the global molecule.

The relatively sparse resonances H4, H20, and H22 of VST were chosen to calculate the average self-diffusion coefficient of conformers A and B. The observed D values were independent of the VST concentration (Table. S2), indicating no self-aggregation occurring in both sample groups. In phosphate buffer, the D values of conformer A and B were 3.59×10^{-10} and 3.44×10^{-10} m^2/s, respectively. After the addition of DPC, the values of conformers A and B dropped to 0.97×10^{-10} and 0.96×10^{-10} m^2/s, respectively (Figure 3). The D value of the VST–DPC complex was larger than that of the DPC alone, 0.49×10^{-10} m^2/s, which was the result of fast exchange

dx.doi.org/10.1021/jp304304v | J. Phys. Chem. B 2012, 116, 7470–7478

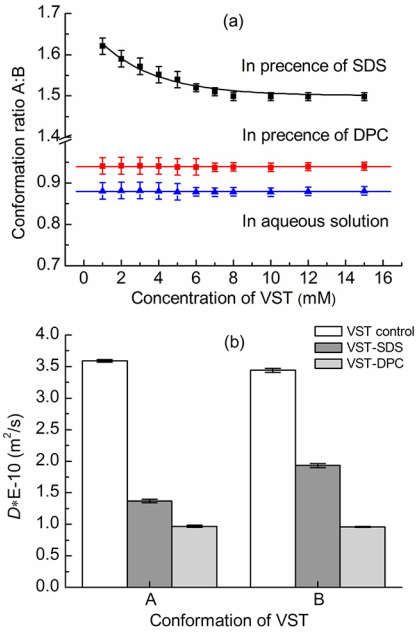

Figure 3. (a) Concentration ratio A:B of VST as a function of VST concentrations. The error bars were calculated by the average conformational integral ratio of H4 and H3 for VST control and H4 and H22 for VST−detergent systems, respectively. (b) Self-diffusion coefficients (D) of the two VST conformers in phosphate buffer (white), 200 mM SDS (gray) and 200 mM d38-DPC micelles (light gray). The error bars were calculated by the average D value of H4 and H3 for VST control, H4 and H22 for the VST−SDS system, and H4, H20, and H22 for the VST−DPC system, respectively.

between free VST and bound ones. We supposed that the molecular size of the DPC micelle does not change much after the binding of VST, so the D value of DPC can be used as D_b. If we take the D value of VST in phosphate buffer as D_f, an increased solvent viscosity has to be taken into account because of the addition of detergent. We measured the self-diffusion coefficients of the residual HOD signals of 99.8% D_2O, which can be observed in the ^{1}H NMR spectra without water suppression. The average D value of residual HOD in free VST samples was 1.90×10^{-9} m^2/s. It reduced to 1.44×10^{-9} m^2/s in the presence of DPC. According to the Stokes−Einstein equation, D_f can be used in eq 4 by multiplying a viscosity coefficient of η_f/η_b, 0.758. Therefore, the bound fraction of VST X_b was calculated to be 78.5% for conformer A and 77.8% for conformer B, respectively.

2. Comparison of the Interaction between VST−DPC and VST−SDS. *NMR Parameters.* The perturbations of NMR parameters demonstrated that VST has strong interactions with DPC and two conformers have almost the same binding affinities with DPC micelles based on the changes of chemical shifts, proton relaxation times and self-diffusion coefficients. This phenomenon was different from the VST−SDS system, where we found that conformer A has obviously higher binding affinity to SDS micelles than conformer B.

We measured the concentration ratio of conformer A to B by the integration of H4 and H22 peaks for VST−detergents systems and the integration of H4 and H3 peaks for VST control (Figure 3a). The ratio fluctuates around 0.88 in the free VST sample. It increases to 0.94 in DPC and reaches 1.50 in SDS. The average self-diffusion coefficient values of both conformers are illustrated in Figure 3b as well. Compared to the control sample, the D values of VST−DPC complexes reduced much more significantly than those of VST−SDS, suggesting a higher binding affinity between VST and DPC. Furthermore, we calculated the X_b of conformers A and B in the VST−SDS systems on the condition that the average D value of residual HOD in the presence of SDS was 1.77×10^{-9} m^2/s and the D value of SDS alone was 0.59×10^{-10} m^2/s, which are 71.7% and 48.7%, respectively. These results quantitatively confirmed that VST has stronger binding affinity with the DPC micelles and higher conformational selectivity in the SDS micelles.

Molecular Dynamics Simulation. NMR experiments provide robust evidence that two VST conformers have different affinities to DPC and SDS micelles. MD simulation was used to find out the inherent binding mechanisms of these two systems.

As the VST−SDS system has been described in detail in our previous work,[20] here we focus on the VST−DPC system. Two MD simulations were carried out for each VST conformer in DPC micelle, respectively. The distances between the center of mass of VST and the micelles were calculated to monitor whether VST has diffused to the interfacial region between micelles and water. For the VST−DPC system, the diffusion finished within 6 ns for conformer A and 5 ns for conformer B (Figure S2), respectively. The values of radius of gyration (R_g) of both systems were 16.7 ± 0.5 Å, which were in good agreement with the previously theoretical value of 17.4 Å[27] and the experimental observations of 16.2 Å[37] and 13.5 to 18.5 Å.[38] It showed that the DPC micelle geometry predicted by the simulation was reliable and comparable to other experiments.

The root-mean-square deviations (rmsd) of VST in the DPC micelle during the simulations were calculated with respect to its initial structure (Figure S3). The rmsd of conformer A fluctuated between 1 and 3 Å during the entire 20 ns simulation; however, rmsd of conformer B remained at 2 Å for the first 13 ns, then reached to 3 Å, and kept stable at this level for the remainder of the simulation. The same phenomena were observed in the VST−SDS system, except that the change of rmsd took place at 11 ns. This indicated that conformer B could have a conformational change on the interface between micelle and water. It also showed that conformer B was more flexible in both micelles.

Five dihedral angles ($\tau1-\tau5$) were defined to describe the structures of conformers A and B in DPC (Figure S4). The five dihedral angles of conformer A remained constant during the simulation. For conformer B, $\tau1$, $\tau2$, and $\tau5$ had no changes. $\tau3$ had a disordered structural change during 5 and 13 ns and kept stable after 13 ns. $\tau4$ shifted about 180° at 13 ns. Similarly, in our previous work of the SDS system, conformer B had major changes in dihedral angle $\tau3$ and $\tau4$ after 11 ns, and conformer A did not show big changes.[20]

Structure Details of the VST−SDS and VST−DPC Complexes. The simulation snapshots in DPC micelles were illustrated in Figure 4. The final structures of two VST conformers showed similar binding conformations with DPC micelles. The carboxyl group is close to the tetrazole ring and the butyl chain is far from these hydrophilic groups. Conformer A almost maintained the initial structure, whereas conformer B had a rotated butyl chain which was still pointing away from the biphenyl rings. Another but important difference is, the tetrazole ring of conformer A was parallel to the micelle surface, while that of conformer B was perpendicular to the micelle surface. The 90 degrees rotation of the molecule

dx.doi.org/10.1021/jp304304v | J. Phys. Chem. B 2012, 116, 7470−7478

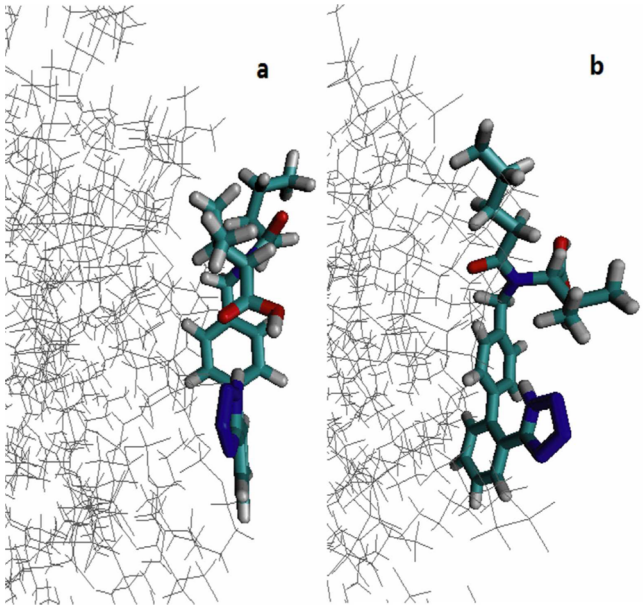

Figure 4. Simulation snapshots of VST, conformer A (a) and conformer B (b), in DPC micelles. The snapshots were all taken at 20 ns. Water molecules were not shown for clarity. VST is color-coded by atom type and DPC detergents are shown in gray bond format.

facilitated the hydrophobic contacts between the biphenyl rings of conformer B and the lipid chain of DPC micelle.

The calculated structures of VST in DPC agreed well with our experimental NOE data. The NOESY spectrum of VST with d38-DPC showed clear NOE cross peaks between the phenyl H13−17 and H7−9 neighboring the carboxyl group in both conformers. Meanwhile, the cross peaks between phenyl H13−17 and H4 were only observed in conformer A, which was consistent with the upfield chemical shift of H4 in conformer A.

Moreover, one can find that the location of VST molecule was at the charged head groups and upper part of the DPC micelles, which agrees well with the Raman spectroscopic studies of VST in the bilayers consisting of zwitterionic detergent DPPC.[12]

Relative Binding Free Energy. In order to identify which conformer of VST has higher affinity in binding to the micelles, the MM/PBSA method was carried out to calculate the relative binding free energy for two conformers of VST with DPC and SDS micelles, respectively. Since the MM/PBSA energy estimates and ranking are reliable only if the average energies are converged, which is conditional upon adequate conformational sampling and may require longer MD trajectories,[39,40] we carried out the sampling of last 4 ns of the whole 20 ns trajectory. Table 1 lists the "relative" free energy changes ($\Delta\Delta G$) of VST isomerization in DPC or SDS systems, including ΔH, $-T\Delta S$, and ΔG_{bind} for VST_A-DPC, VST_B-DPC, VST_A-SDS, and VST_B-SDS systems, respectively. Here, the term "relative" refers the differences in binding energy between two conformers of VST in the detergents (DPC and SDS)

$$\Delta\Delta G = \Delta G_{VST_A} - \Delta G_{VST_B} \quad (6)$$

If $\Delta\Delta G < 0$, it means the VST_A will be the preferable conformer in the micelle system; otherwise, VST_B will be. For VST−SDS systems, the value of $\Delta\Delta G$ was −1.53 kcal/mol which was in good agreement with the value of −0.6725 kcal/mol calculated by thermodynamic cycle method in our previous study.[20] On the other hand, for VST-DPC, the value of $\Delta\Delta G$ was 0.72 kcal/mol which was predicated that VST_A binds 0.72 kcal/mol weaker to DPC micelle than VST_B. These calculated results were well consistent with the present experimentally observed results.

3. Hydrophobic and Electrostatic Interaction between VST and Other Detergents. The different behaviors of the binding affinity of two VST conformers in SDS and DPC stimulated us to do further investigations. SDS shares the same lipid chain but different ionic headgroup with DPC. In our experimental condition (pH 7.4), the headgroup of SDS is negatively charged, whereas the choline headgroup of DPC has a positively charged surface. The carboxyl and amidocyanogen groups of valsartan are negatively charged.[41] So it can be reasonably assumed that the electrostatic interaction should play an important role in helping valsartan insert into the DPC micelles. If that is the case, two VST conformers should have similar binding affinities when binding to cationic or zwitterionic detergents other than DPC. Based on this assumption, cationic detergent CTAB and nonionic detergent Tween-20 were chosen according to their hydrophilic groups. Since the changes of NMR parameters are independent of VST concentration, only one sample containing 15.0 mM VST was tested for each detergent. The concentrations of these detergents used in our experiments are far above their CMCs to form stable micelles (Table S3).

Chemical shift drifting and line broadening can be clearly observed in Figure 1 with the addition of various detergents. Proton relaxation times and self-diffusion coefficients were listed in Table 2. Obviously, both conformers have interactions with these detergents. The reducing amplitudes of T_2 relaxation times and self-diffusion coefficients differ a lot between conformer A (T_2, 64.0%; D, 57.8%) and B (T_2, 49.5%; D, 42.7%) in SDS. In contrast, these values are almost the same for two conformers in CTAB (T_2, about 80%; D, about 40%) or DPC (T_2, about 80%; D, about 70%).

To get more detailed binding information, we recorded 2D NOESY spectra for VST in all detergents. The intensity of the cross peak in the NOESY spectrum is inversely proportional to

Table 1. Binding Free Energies of Two Conformers of VST with DPC and SDS Micelles[a]

system	ΔG_{mmpbsa}	$-T\Delta S_{tot}$	ΔG_{bind}	$\Delta\Delta G$	ΔG_{theor}
VST_A−DPC	−29.65(0.20)	25.46(1.40)	−4.19(1.40)		
VST_B−DPC	−29.78(0.21)	24.87(1.68)	−4.91(1.68)		
VST_A−SDS	−33.27(0.39)	29.47(1.60)	−3.80(1.60)		
VST_B−SDS	−29.87(0.50)	27.60(1.17)	−2.27(1.17)		
VST−DPC				0.72	
VST−SDS				−1.53	−0.6725[b]

[a]Mean contributions are in kcal/mol, with corresponding standard deviations in parentheses. [b]Data from ref 16.

dx.doi.org/10.1021/jp304304v | J. Phys. Chem. B 2012, 116, 7470−7478

Table 2. NMR Parameters Perturbations of 15.0 mM VST in Different Solvents

	T_1 (s)			T_2 (s)			$D \times 10^{-10}$ m^2/s			A:B	
solvent	14/16B	4B	4A	14/16B	4B	4A	14/16B	4B	4A	22	4
PB	1.86	0.55	0.56	0.782	0.283	0.311	3.40	3.63	3.32	0.88[a]	0.87
CTAB	0.97	0.55	0.55	0.121	0.052	0.045	1.83	1.98	1.88	0.96	0.94
DPC	1.57	0.53	0.50	0.151	0.057	0.062	0.98	1.01	1.00	0.94	0.93
Tween-20	1.12	1.34[b]	1.32[b]	0.153	0.171[b]	0.152[b]	0.77	0.81[b]	0.59[b]	1.20	1.22[c]
SDS	1.50	0.54	0.53	0.310	0.143	0.112	2.17	2.08	1.40	1.51	1.49

[a]Data calculated from H3 proton. [b]NMR parameters calculated from H22 proton. [c]Data calculated from H13−17 proton.

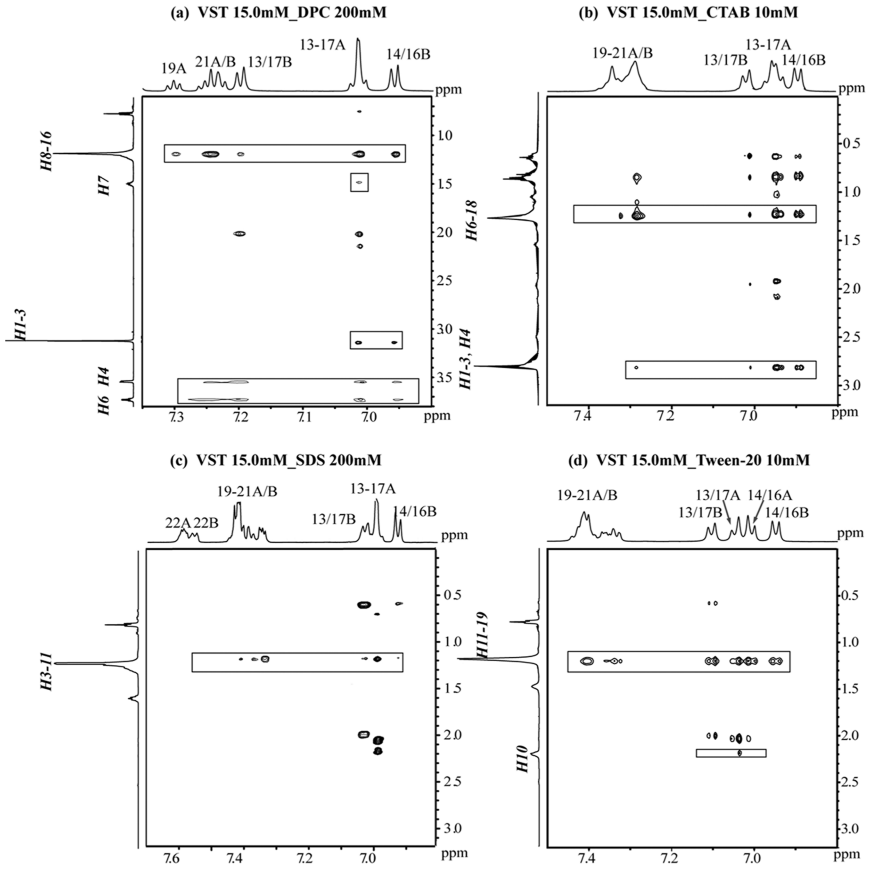

Figure 5. Expansions of NOESY spectra of 15.0 mM VST in 200 mM DPC (a), 10 mM CTAB (b), 200 mM SDS (c), and 10 mM Tween-20 (d). The mixing time is 200 ms. Intermolecular cross peaks are indicated with rectangles and the protons of VST and detergents involved in the interaction are labeled in normal and italic fonts, respectively.

the distance between the paired protons to the sixth power. In Figure 5a, it can be clearly seen that both conformers interact with DPC through not only the hydrophobic lipid chain but also the methyl and methylene protons adjacent to the choline headgroup. The same phenomenon can be observed in Figure 5b, where CTAB showed NOE cross peaks with two VST conformers through both the aliphatic chain and the methyl and methylene protons adjacent to the choline headgroup. In Figure 5, panels c and d, we only observed the NOE cross peaks between VST and the lipid chain of SDS or Tween-20. No NOEs were found between VST and the protons adjacent to the head groups. On the other hand, we measured the average concentration ratio of conformer A to B in CTAB and Tween-20, which were 0.95 and 1.21, respectively (Table 2). When arranging all of these detergents according to an increasing concentration ratio of A to B, the order would be phosphate buffer < cationic (CTAB), zwitterionic (DPC) < nonionic (Tween-20) < anionic detergent (SDS), which is in agreement with the charge characters of these detergents. The NOESY spectra and results of the concentration ratio indicated that the interaction mode of VST and its binding affinity to the detergents are highly dependent on the type of hydrophilic groups of the micelles. For DPC, VST anchors at the headgroup and upper segment of the micelle and maintains the conformation in aqueous solution. For SDS, VST inserts deeply into the micelle and shows high conformational selectivity.

CONCLUSIONS

In this paper, we investigated the interactions between VST and various detergents by NMR techniques and MD simulations. We found that both conformers have interactions with micelles, but the binding affinity is highly correlated with the charge characters of the detergents.

In DPC and CTAB, two conformers have similar binding conformations and binding affinities. NOE cross peaks were

dx.doi.org/10.1021/jp304304v | J. Phys. Chem. B 2012, 116, 7470−7478

found between the aromatic protons of VST and the methyl and methylene protons adjacent to the choline head groups. It suggests that the drug locates on the micelle surface where the electrostatic interaction plays an important role in drawing the negatively charged tetrazole ring and partially positively charged choline head groups together. Hydrophobic interaction also exits in the binding process to increase the stabilities of the complexes demonstrated by the NOE observations. However, in SDS, the negatively charged head groups are unfavorable for the binding of VST. Once inserting into the micelles, the hydrophobic interaction becomes the predominant effect which selects the better hydrophobic packing of VST conformation. Conformer A has a more concentrated hydrophobic core and is easier to insert into the micelles, whereas conformer B has to change its conformation to enhance the hydrophobic interactions which requires a higher binding free energy. The same thing happens for Tween-20. Its nonionic headgroup causes the hydrophobic interaction to be the only favorable effect to help the drug penetrate into the micelles. Conformer A becomes the preferred conformation.

In conclusion, VST adopts different binding modes in different detergents because of its negatively charged tetrazole ring. For the detergents having positively charged head groups, the electrostatic interaction plays an essential role in the binding process. For the negatively charged detergents, the hydrophobic interaction is the predominant effect. Thus, it can be reasonably assumed that in the physiological environment the electrostatic attractions help VST anchor on the surface of the cell membrane and then the hydrophobic interactions promote the penetration of VST into the cell membrane. Finally, VST reaches the transmembrane binding pocket of the AT_1 receptor and triggers a series of signal transductions and cell responses. Therefore, as one of the wildly clinically used sartan drugs, VST provides us an ideal sample for the investigation on the drug conformational changes in the membrane mimicking environment. The efficiency of the drug delivery highly depends on the distribution of charged and hydrophobic groups of the molecule. The results facilitate the understanding of the delivery mechanism of sartan drugs in biological membranes and provide insights into the drug design for the hypertension treatment.

■ ASSOCIATED CONTENT

Supporting Information

Relaxation times for valsartan protons in the absence and presence of 200 mM d38-DPC (Table S1); self-diffusion coefficients of valsartan protons in the presence of 200 mM d38-DPC (Table S2); critical micelle concentrations of detergents and concentrations used in the experiments (Table S3); expanded NOESY spectrum of VST in the presence of d38-DPC (Figure S1); distance between the center of mass of DPC micelle and VST (Figure S2); root mean square deviations (rmsd) of carbon atoms of VST relative to its initial structure (Figure S3); time profiles of dihedral angles τ1, τ2, τ3, τ4, and τ5 of VST during the simulation (Figure S4). This material is available free of charge via the Internet at http://pubs.acs.org.

■ AUTHOR INFORMATION

Corresponding Author

*E-mail: lingjiang@wipm.ac.cn (L.J.); hehq@wipm.ac.cn (H.H.).

Notes

The authors declare no competing financial interest.

■ ACKNOWLEDGMENTS

We acknowledge Prof. Yuqi Feng (College of Chemistry and Molecular Sciences, Wuhan University) for providing us valsartan. This work is supported by grants from National Major Basic Research Program of China (No. 2009CB918603) and National Science Foundation of China (Nos. 90813017, 20833007, and 21173257).

■ REFERENCES

(1) Criscione, L.; Bradley, W. A.; Buhlmayer, P.; Whitebread, S.; Glazer, R.; Lloyd, P.; Mueller, P.; Gasparo, M. *Cardiovasc. Drug Rev.* **1995**, *13*, 230−250.
(2) Wang, J.; et al. *J. Clin. Invest.* **2007**, *117*, 3393−3402.
(3) Li, N. C.; Lee, A.; Whitmer, R. A.; Kivipelto, M.; Lawler, E.; Kazis, L. E.; Wolozin, B. *Brit. Med. J.* **2010**, *340*, b5465.
(4) Mukoyama, M.; Nakajima, M.; Horiuchi, M.; Sasamura, H.; Pratt, R. E.; Dzau, V. J. *J. Biol. Chem.* **1993**, *268*, 24539−24542.
(5) Murphy, T. J.; Alexander, R. W.; Griendling, K. K.; Runge, M. S.; Bernstein, K. E. *Nature* **1991**, *351*, 233−236.
(6) Zoumpoulakis, P.; Daliani, I.; Zervou, M.; Kyrikou, I.; Siapi, E.; Lamprinidis, G.; Mikros, E.; Mavromoustakos, T. *Chem. Phys. Lipids* **2003**, *125*, 13−25.
(7) Theodoropoulou, E.; Marsh, D. *Biochim. Biophys. Acta* **1999**, *1461*, 135−146.
(8) Theodoropoulou, E.; Marsh, D. *Biochim. Biophys. Acta* **2000**, *1509*, 346−360.
(9) Fotakis, C.; Christodouleas, D.; Zoumpoulakis, P.; Kritsi, E.; Benetis, N. P.; Mavromoustakos, T.; Reis, H.; Gili, A.; Papadopoulos, M. G.; Zervou, M. *J. Phys. Chem. B* **2011**, *115*, 6180−6192.
(10) Hodzic, A.; Zoumpoulakis, P.; Pabst, G.; Mavromoustakos, T.; Rappolt, M. *Phys. Chem. Chem. Phys.* **2012**, *14*, 4780−4788.
(11) Ntountaniotis, D.; Mali, G.; Grdadolnik, S. G.; Maria, H.; Skaltsounis, A. L.; Potamitis, C.; Siapi, E.; Chatzigeorgiou, P.; Rappolt, M.; Mavromoustakos, T. *Biochim. Biophys. Acta* **2011**, *1808*, 2995−3006.
(12) Potamitis, C.; Chatzigeorgiou, P.; Siapi, E.; Viras, K.; Mavromoustakos, T.; Hodzic, A.; Pabst, G.; Cacho-Nerin, F.; Laggner, P.; Rappolt, M. *Biochim. Biophys. Acta* **2011**, *1808*, 1753−1763.
(13) Vinogradova, O.; Sonnichsen, F.; Sanders, C. R., II *J. Biomol. NMR* **1998**, *11*, 381−386.
(14) Garavito, R. M.; Ferguson-Miller, S. *J. Biol. Chem.* **2001**, *276*, 32403−32406.
(15) Gong, Q.; Menon, L.; Ilina, T.; Miller, L. G.; Ahn, J.; Parniak, M. A.; Ishima, R. *Chem. Biol. Drug Des.* **2010**, *77*, 39−47.
(16) Delfini, M.; Gianferri, R.; Dubbini, V.; Manetti, C.; Gaggelli, E.; Valensin, G. *J. Magn. Reson.* **2000**, *144*, 129−133.
(17) Bernardi, F.; Gaggelli, E.; Molteni, E.; Porciatti, E.; Valensin, D.; Valensin, G. *Biophys. J.* **2006**, *90*, 1350−1361.
(18) Qin, X.; Liu, M.; Yang, D.; Zhang, X. *J. Phys. Chem. B* **2010**, *114*, 3863−3868.
(19) Li, F.; Zhang, H.; Jiang, L.; Zhang, W.; Nie, J.; Feng, Y.; Yang, M.; Liu, M. *Magn. Reson. Chem.* **2007**, *45*, 929−936.
(20) Li, F.; Wang, L.; Xiao, N.; Yang, M.; Jiang, L.; Liu, M. *J. Phys. Chem. B* **2010**, *114*, 2719−2727.
(21) Potamitis, C.; et al. *J. Chem. Inf. Model.* **2009**, *49*, 726−739.
(22) Nie, J.; Xiang, B.; Feng, Y.; Wang, D. *J. Liq. Chromatogr. Relat. Technol.* **2006**, *29*, 553−568.
(23) Mao, J.; Jiang, L.; Jiang, B.; Liu, M.; Mao, X. *J. Magn. Reson.* **2010**, *206*, 157−160.
(24) Bertmer, M.; Eckert, H. *Solid State Nucl. Magn. Reson.* **1999**, *15*, 139−152.
(25) Liu, M.; Mao, X.; Ye, C.; Huang, H.; Nicholson, J. K.; Lindon, J. C. *J. Magn. Reson.* **1998**, *132*, 125−129.

(26) Case, D. A.; et al. *AMBER 10*; University of California: San Francisco, CA, 2008.
(27) Wang, J.; Wolf, R. M.; Caldwell, J. W.; Kollman, P. A.; Case, D. A. *J. Comput. Chem.* **2004**, *25*, 1157−1174.
(28) Chen, J. M.; Su, T. M.; Mou, C. Y. *J. Phys. Chem.* **1986**, *90*, 2418−2421.
(29) Wymore, T.; Gao, X. F.; Wong, T. C. *J. Mol. Struct.* **1999**, *485*−*486*, 195−210.
(30) Frisch, M. J.;et al. *Gaussian 09*, revision A.1; Gaussian, Inc: Wallingford, CT, 2009.
(31) Fox, T.; Kollman, P. A. *J. Phys. Chem. B* **1998**, *102*, 8070−8079.
(32) Humphrey, W.; Dalke, A.; Schulten, K. *J. Mol. Graph.* **1996**, *14*, 33−38.
(33) Gilson, M. K.; Sharp, K. A.; Honig, B. H. *J. Comput. Chem.* **1988**, *9*, 327−335.
(34) Sitkoff, D.; Sharp, K. A.; Honig, B. *J. Phys. Chem.* **1994**, *98*, 1978−1988.
(35) Sanner, M. F.; Olson, A. J.; Spehner, J. C. *Biopolymers* **1996**, *38*, 305−320.
(36) Stilbs, P. *Prog. NMR Spec.* **1987**, *19*, 1−45.
(37) Gao, X.-F.; Wong, T. C. *Biophys. J.* **1998**, *74*, 1871−1888.
(38) Lauterwein, J.; Bosch, C.; Brown, L. R.; Wuthrich, K. *Biochim. Biophys. Acta* **1979**, *556*, 244−264.
(39) Pearlman, D. A. *J. Med. Chem.* **2005**, *48*, 7796−7807.
(40) Lu, Y.; Yang, C. Y.; Wang, S. *J. Am. Chem. Soc.* **2006**, *128*, 11830−11839.
(41) Flesch, G.; Müller, P.; Lloyd, P. *Eur. J. Clin. Pharmacol.* **1997**, *52*, 115−120.